PERGAMON

Computerized Medical Imaging and Graphics 23 (1999) 181–191

Computerized Medical Imaging and Graphics

www.elsevier.com/locate/compmedimag

Analysis of dynamic nuclear cardiac images by covariance function

A.-O. Boudraa[a,b,*], J. Champier[c], M. Djebali[d], F. Behloul[e], A. Beghdadi[a]

[a]*L2TI, Institut Galilée, Université Paris XIII, J.B. Clément, Villetaneuse 93430, France*
[b]*CREATIS, CNRS UMR 5515 Affiliated to INSERM, INSA-502, 69621 Villeurbanne, France*
[c]*Laboratoire de Biophysique, Faculté de Médecine René Laennec, rue Guillaume Paradin, 69372 Lyon Cedex 08, France*
[d]*LIGIA-LISPI, Université Lyon I, Bat. 710, 43 Bd 11 Novembre 1918, 69622 Villeurbanne, France*
[e]*Division of Image Processing (LKEB), Department of Radiology, Leiden University Medical Center PO Box, 9600, 2300 RC Leiden, The Netherlands*

Received 26 August 1998; accepted 23 April 1999

Abstract

A new method using the covariance function as a measure of functional similarity is presented for dynamic analysis of a sequence of scintigraphic cardiac images taken throughout the cardiac cycle. The similarity between the temporal response of pixels in a reference region of the scintigraphic image series and the temporal response of the remaining pixels in the image sequence is calculated. The resulting covariance image is a functional image representing regions with different temporal dynamics. A box-plot representation of this image permits better interpretation for clinical decision making. This analysis allows visualization of the ventricular emptying pattern, which may be useful in studying motion or conduction abnormalities. Compared to Fourier analysis, our method does not make assumption that the data are periodic and that the transition between the first and the last frame of the study is smooth. The proposed method has been performed in one normal patient and twenty patients with abnormal ventricular contraction patterns, and there is no computational difficulty in its implementation. A comparison with the Fourier analysis is performed.

Keywords: Radionuclide ventriculography; Covariance function; Pattern recognition; Time series analysis; Ventricular function

1. Introduction

Gated blood pool scintigraphy is a reliable non-invasive method for detecting abnormalities of contraction and conduction [1]. This imaging technique provides a time sequence of images taken throughout the whole cardiac cycle. The images demonstrate temporal changes in radioactive tracer distribution. The quantitative information contained in the images describes the physiological behaviour of the imaged structures such as the left ventricle (LV) and the right ventricle (RV). Conventional analysis of such series of images is usually performed by visual evaluation of differences from image to image in order to obtain qualitative information about the cardiac contraction kinetics. This is not the optimal way to interpret the changes appearing in the images along the series. Therefore, image processing methods designed to extract as much biomedical/diagnostic information as possible and to ease clinical interpretation have been developed: the standard functional imaging methods using the ejection fraction (EF) or the stroke volume images are commonly used. The EF image colour codes the end diastolic frame in terms of regional EF [2], while the stroke volume colour codes the end diastolic frame in terms of regional stroke volume [3]. These types of images have been useful in the past and are still so [2,3], but they have some limitations [4]. For example, their dependence upon an accurate choice of the end systolic frame as well as poor single frame statistics. Furthermore, their appearance is influenced by cardiac anatomy, even in normal hearts, and by the surrounding structures. Based on the first harmonic fit to the pixel time activity curve, Fourier analysis [5] has also been used to detect and describe wall motion abnormalities [6,7]. The primary assumption of Fourier analysis is that the data are periodic and the second is that the transition between the first and the last frame of the study must be smooth. This analysis generates two parametric images, the amplitude image corresponding to the maximal changes in counts within the image series regardless of the time these changes appear and the phase image corresponding to the time of maximal contraction (end-systole). In a first approximation, the amplitude image is proportional to the stroke volume. The phase image allows good separation of the ventricular regions (left or right) from the atria and this processing is useful to delineate automatically the LV

* Corresponding author. Tel.: + 33-149-404062; fax: + 33-149-403366.

E-mail address: abdel.boudra@l2ti.univ-paris13.fr (A.-O. Boudraa)

0895-6111/99/$ - see front matter
PII: S0895-6111(99)00017-8

contours in order to estimate the EF value from ventricular regions of interest [8]. Compared to the standard method, Fourier analysis does not depend upon the precise choice of the end systolic frame and is not influenced by the heart morphology and its adjacent structures [9]. However, Fourier analysis has also some limitations. The absolute times indicated by the first harmonic phase do not correspond to the onset of contraction but to the end of contraction. The phase is moreover influenced by the shape of the entire time activity curve. Some clinical limitations have been stressed, particularly in cases of severely impaired left ventricular function [10] and in the akinetic or severely hypokinetic segments where the phase values are uncertain [11]. In spite of the apparent mathematical difficulties, factor analysis has gained clinical acceptance for cardiac studies at equilibrium with abnormalities of both contraction and conduction [12,13]. This analysis assumes that any time activity curve is a weighted sum of a limited number of pure time activity evolutions, called physiological components [13]. These components correspond to regions of similar temporal behaviour. The estimated physiological components given by this analysis are used to reconstruct true function images (factor images). This method has an obvious similarity with Fourier analysis: while Fourier analysis is based on sine and cosine functions, no such restriction is placed on the shape of the principal components. Although factor analysis provides a valid representation of wall motion and conduction abnormalities, some limitations must be considered. The quality of the results and the number of significant factors depend on the signal to noise ratio of the dynamic series [13]. Furthermore, the criteria used for the interpretation must be refined [14,15]. This perhaps avoids the need to make conclusions based on activity curves of "unphysiologic" shape.

In this paper, a new technique designed to analyse nuclear cardiac image series is proposed. Compared to Fourier analysis this method does not make assumption that the data are periodic or no restriction is placed on the shape of the pixel time activity curve. This method segments the time series of the cardiac images in regions of similar temporal behaviour (components) but, contrary to principal components analysis, we do not need to know their number to start the method The aim of this technique is to capture the essential of the sequence while reducing the amount of image data presented to the clinician for diagnostic interpretation. This method is based on the measure of similarity between the temporal response of pixels in a reference region of interest (ROI) and the temporal response of the other pixels in the image series. The calculated similarity provides quantitative information about the degree of local similarity in comparison with the ROI taken as a reference.

2. Method

2.1. Mathematical description of the covariance method

Template matching is perhaps the most straightforward way of locating the presence of an object of interest within an image field. The template is a duplicate of the sought object. If the template matches between an unknown object and if it is sufficiently close, the unknown object is labelled as the template object. In nuclear cardiac studies, the template is a fixed reference time activity curve describing the temporal evolution of a cardiac ROI during the cardiac cycle. The image field to be searched is the time series of cardiac images. For dynamic analysis, template matching may be viewed as a temporal one. For example, the template may therefore be a time activity curve of a sub-region of the LV or the whole ventricle. Similarity measures provide quantitative means of determining the degree of temporal match between the time sequence of images and the template. The similarity may be performed by several similarity functions such as the cross-correlation [16,17], the sum of absolute valued difference (SAVD) [18], the covariance function [19], the Tanimoto coefficient [20] and the stochastic sign change (SSC) criterion [21]. The SSC criterion and the SAVD are computationally more economical than the correlation coefficient. A comparison of these similarity measures to register a template in a sequence of near-infrared eye images was performed by Wagner and Galiana [22].

Let us denote by $\mathrm{AC}(i,j,t)$, $(t = 1,\ldots,T)$, the time activity of the (i,j)-th pixel, where T is the number of images in the series. T is also the cardiac cycle duration. The covariance value of the *(i,j)*-th pixel is given by

$$\mathrm{Cov}(i,j) = \frac{1}{T}\sum_{t=1}^{T}(\mathrm{AC}(i,j,t) - \mu_{\mathrm{AC}}(i,j))(R(t) - \mu_{\mathrm{R}})$$

$$R(t) = \frac{1}{M}\sum_{(i,j)\in \mathrm{ROI}}\mathrm{AC}(i,j,t)$$

$$\mu_{\mathrm{R}} = \frac{1}{T}\sum_{t=1}^{T}R(t)$$

$$\mu_{\mathrm{AC}}(i,j) = \frac{1}{T}\sum_{t=1}^{T}\mathrm{AC}(i,j,t)$$

where $R(t)$ is the reference series, μ_{R} the mean value of the reference series and $\mu_{\mathrm{AC}}(i,j)$ the mean value of the time activity curve of the (i,j)-th pixel. M is the total number of pixels in the ROI. There is no major problem of spatial registration for this kind of images because the images of the series correspond to the same morphologic projection even if its shape changes with time.

The method is based on the computation, pixel by pixel, of the covariance $\mathrm{Cov}(i,j)$ between two time series

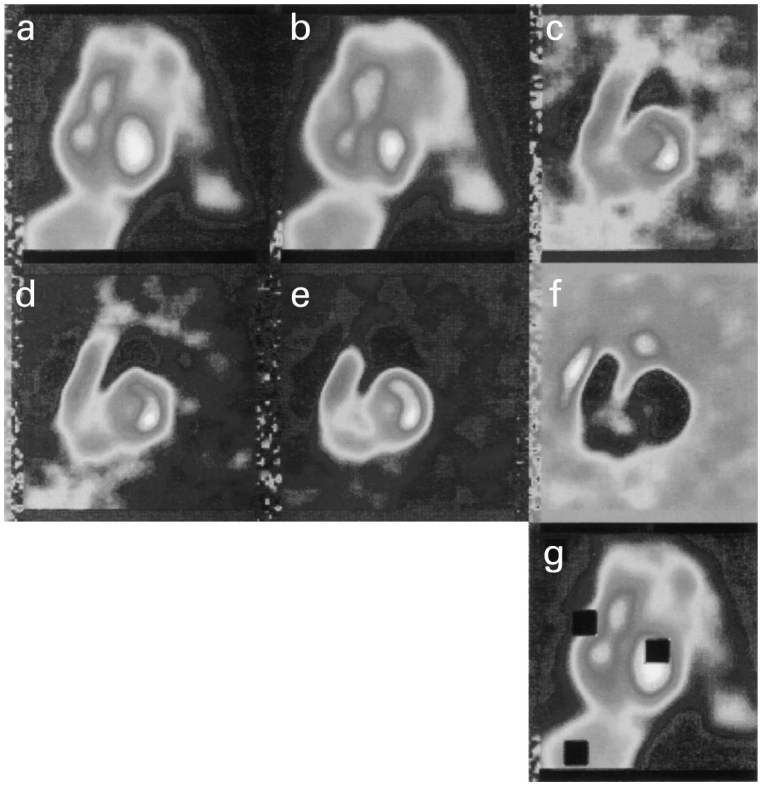

Fig. 1. Study of the normal patient. (a) End-diastolic image; (b) end-systolic image; (c) covariance map of the background ROI reference; (d) covariance map of the liver ROI reference ; (e) covariance map of the LV ROI reference; (f) covariance map of the atria ROI reference; (g) end-diastolic image with the reference ROIs of the background (top left), the liver (bottom left), the LV (middle right) and the atria (middle left).

representing the time activity curve of any pixel and a reference time series. The generated similarity map is an image where the value of each pixel represents the degree of temporal similarity to the reference. This similarity measure is less than $\sigma_{AC}\cdot\sigma_R$ in absolute value where σ_{AC} and σ_R are the standard deviations of the time activity curve and the reference, respectively. A positive value of the covariance indicates that the time activity curve and the reference variables vary in the same sense. While, a negative value indicates that these two variables vary in opposite sense. It is important to keep in mind that all the pixels that match or mismatch the reference are equally important to describe or to interpret the information contained in the image series.

2.2. Fourier analysis

Let Sora(i,j,k) be the value of the pixel (i,j) of the kth cardiac image. Two images, respectively, I_{cos} and I_{sin} are calculated using the following equations:

$$I_{cos}(i,j) = \sum_{k=1}^{T} \cos\left[\frac{2\pi}{T}(k-1)\right] \times \text{Sora}(i,j,k)$$

$$I_{sin}(i,j) = \sum_{k=1}^{T} \sin\left[\frac{2\pi}{T}(k-1)\right] \times \text{Sora}(i,j,k)$$

The phase image is given by

$$I_{phase}(i,j) = \arctan\left(\frac{I_{sin}(i,j)}{I_{cos}(i,j)}\right)$$

and the amplitude by:

$$I_{amp}(i,j) = \sqrt{I_{cos}(i,j)^2 + I_{sin}(i,j)^2}$$

The amplitude image is a picture of pixel-by-pixel stroke volume. The rationale for using the phase image rests on the observation that ischemia reduces the velocity of myocardial contraction and thus local abnormalities of wall motion are frequently associated with changes in the time of wall movement.

2.3. Study population and study protocol

The study consists of 21 gated cardiac blood pool examinations analysed by the covariance and the Fourier techniques. Equilibrium gated blood pool scintigrams are obtained after injection of 15–20 mCi (550–740 MBq) of Tc-99m for red blood cells labelling in vivo. The acquisition is performed with a Sopha Medical DS7 gamma camera. Cardiac cycles are divided into 16 (64×64) frames. The imaging is performed in LAO projection. The processing of the cardiac image series is performed on a personal computer and the method implemented in C language. The covariance and Fourier analysis methods are applied

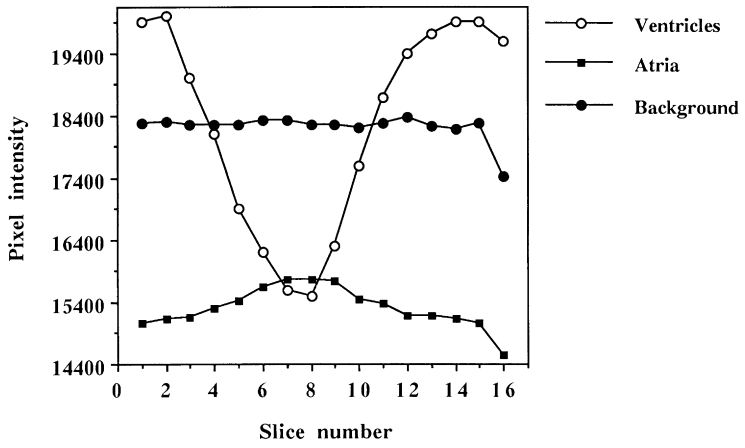

Fig. 2. Physiological curves of the normal patient: (-○-) ventricles, (-■-) atria, (-●-) background.

to the 21 patients but only the images and graphical illustrations of 5 representatives of them are presented (patient 1: normal and patients 2,3,4,5: pathological cases).

2.4. Covariance map

The covariance measure reflects the position of the nadir in a harmonic sinusoidal type curve over the cardiac cycle (R–R interval) expressed in degrees of similarity on a scale ranging from 0 to 200. In theory, the value $-\sigma_{AC}\cdot\sigma_R$ is assigned to a pixel with an opposed temporal behaviour with respect to the mean value of the reference and $+\sigma_{AC}\cdot\sigma_R$ to a pixel having the same temporal response. For more simplicity, the similarity degrees are shifted by + 100 avoiding the negative values. Thus, a similarity degree equal to 100 indicates that there is no temporal similarity between the pixel and the reference. Fig. 1 shows, in the case of a normal patient, the covariance map of the background (Fig. 1(c)), of the liver (Fig. 1(d)), of the LV (Fig. 1(e)) and of the atrium (Fig. 1(f)) ROI references. Each reference time series is calculated in a 5×5 pixels window size of the corresponding ROI. Fig. 1(a) and (b) represent the end diastolic and the end systolic images, respectively.

Once a covariance map is calculated for all pixels, with respect to a reference ROI, its values are mapped into 0 through 255. The map is displayed with a 256 colour look-up table and a colour coded image represents the distribution of the temporal degree of similarity to be assessed. Thus, in an image region having the same temporal evolution, the pixels have the same colour. For example, the ventricles are displayed in red and the atria in blue (Fig. 1(e)). This is expected since the atrial pixels are out of phase with the ventricular ones. This colour coding is inverted in Fig. 1(f), because the reference ROI is placed in a region with temporal behaviour opposed to that of the ventricles. For all reference ROI placements, the red colour corresponds to a maximum covariance value and the blue colour to a minimum one. Like the phase image, the strength

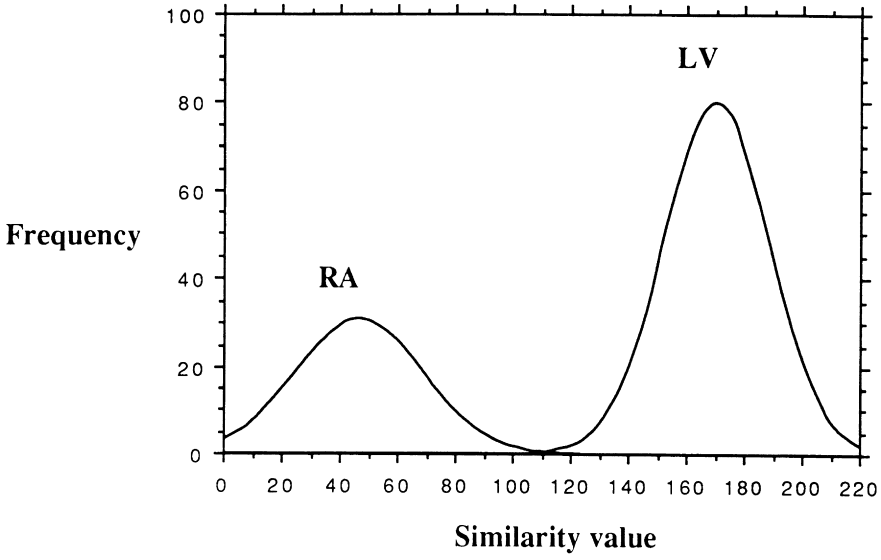

Fig. 3. Gaussian fitted histograms of the similarity values calculated in the right atria and the LV regions for the normal patient.

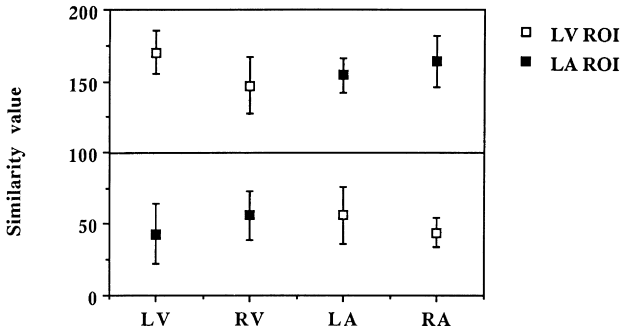

Fig. 4. Mean similarity values calculated in the ventricular and the atrial structures with the reference positioned on the LV and the left atria ROIs in the normal patient.

of the covariance image lies in its relative and not in its absolute values.

2.5. Phase image

In this study we compare the results of the covariance map to those of the phase image. The temporal Fourier transform is obtained on pixel-by-pixel basis. Pixels whose amplitude at the fundamental frequency is above 15% of the maximum amplitude are counted, so that the background does not contribute to the phase image. Pixels less than 15%, usually, correspond to static (extra-cardiac) structures.

3. Results

The results given by the covariance map (Fig. 1(e)) are illustrated in Fig. 2 by the two physiological curves. Note the opposition of the ventricular and atrial curves. A quite typical bimodal similarity histogram showing a significant

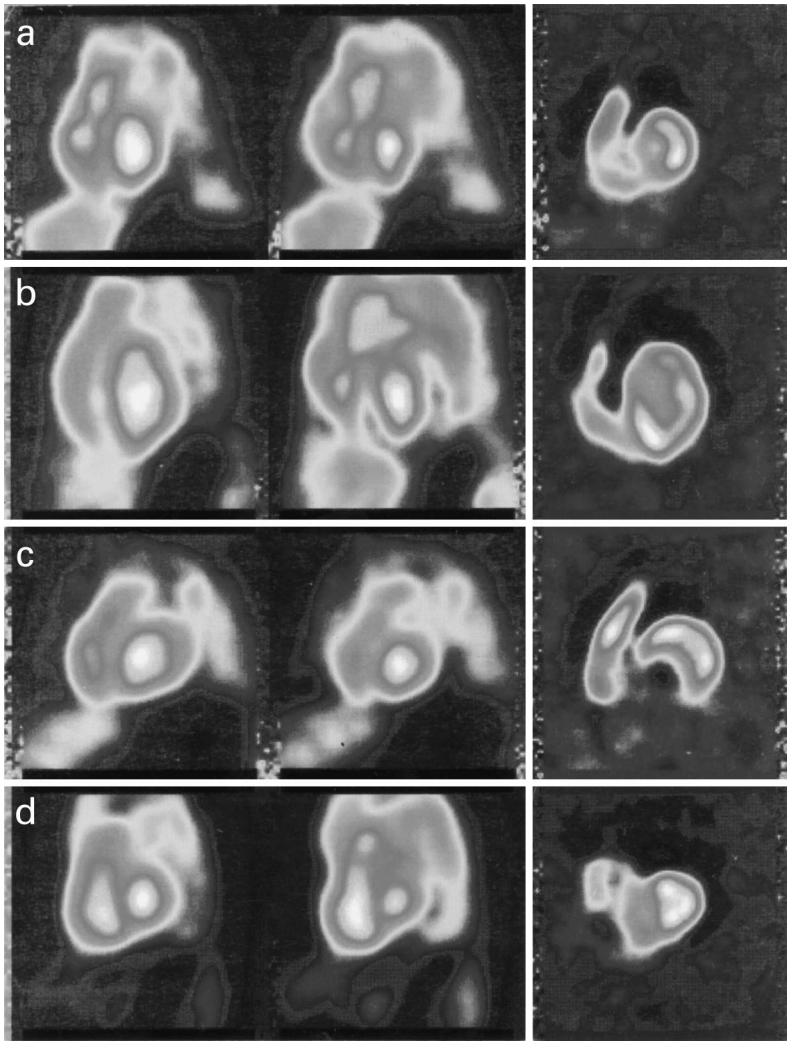

Fig. 5. Study of the four pathological patients (from top to bottom: patients 2–5): (a) end-diastolic image; (b) end-systolic image; (c) covariance map of the LV ROI reference.

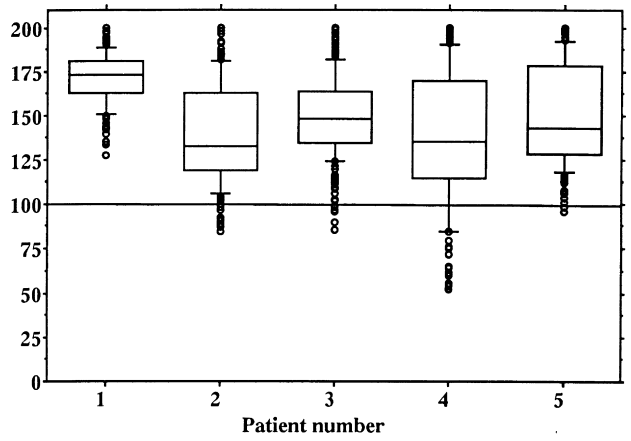

Fig. 6. Box-plot representation of the similarity values distribution calculated in the LV for the five patients (1: normal patient; 2, 3, 4 and 5: pathological patients). The box represents the middle half of the data, the whiskers extend to the extreme values and the line inside the box represents the median.

separation of the LV and the right atrium (RA) of the normal patient is presented in Fig. 3. This histogram is obtained with the ROI reference positioned on the left ventricular region. Thus, the histogram peaks corresponding to RA and the LV are located at 45 and 170, respectively. In contrast, a reference placed on the atrial region leads to an inversion of these two values (Fig. 4). The reference positioned either on the LV or on the RV region was demonstrated to be the best condition to assess the distribution of the temporal degree of similarity in the 21 patients. Fig. 5 shows the results obtained with the reference placed on the LV region for the four pathological cases. As in the normal case, the atria and the ventricles structures are well separated and delimited. From these similarity maps, the same physiological curves, as illustrated in Fig. 2, are obtained. However, even the two peaks of the RA and the LV are separated as in Fig. 3 (normal case), there is an overlap of the Gaussian fitted histograms of these structures. The degree of this overlapping varies from one patient to another. In placing the reference on the atria, we obtain the same inversion of the mean similarity values of the different cardiac structures as illustrated above for the normal case. By comparison with the normal subject, the mean values and the corresponding standard deviations are different due, in part, to some degree of contraction heterogeneity observed in the ventricles of these four patients.

Fig. 5 shows the results obtained in four pathological patients (from top to bottom: patients 2–5). The left and the middle columns represent the end diastolic and systolic images of the four patients, respectively. The corresponding covariance maps are shown in the right column. In patient 2, the similarity map shows the septal portion of the LV with a delayed temporal response compared to the remaining segments of the ventricle (Fig. 5(a)). The lateral segment demonstrates a mean similarity value of 126 ± 16 ($n = 156$ pixels) and the septal segment a mean of 151 ± 29 ($n = 78$ pixels). These two means are significantly different from that in the normal patient: 170 ± 15 ($n = 194$ pixels, $p < 0.005$). Although the LV has a normal morphology, it presents an anteroseptal and apical hypokinesia. Patient 3 has a largely dilated LV (Fig. 5(b)). As previously described, the opposition of the temporal responses of the ventricles and the atria are well demonstrated. As the LV, the RV is dilated but its anterobasal portion is hypokinetic. This portion reveals a mean similarity value of 96 ± 20 ($n = 33$ pixels) while in the normal patient the mean value of the RV is 148 ± 20 ($n = 145$ pixels). Patient 4 also has a dilated LV (Fig. 5(c)). The covariance image reveals, in the LV, an akinesis of the inferoapical segment and a dyskinesis of the distal septum. The last segment presents a mean value of 85 ± 15 ($n = 56$ pixels) and the latter a mean of 52 ± 10 ($n = 25$ pixels), which is not different from that found in the LA region: 49 ± 16 ($n = 146$ pixels, $p > 0.05$). In patient 5 (Fig. 5(d)), the similarity map shows that there is an akinesis of the inferior part of the RV (81 ± 20) ($n = 50$ pixels) with a limited dyskinetic region (73 ± 17, $n = 22$ pixels). One may also note an hypokinesis of the septal segment of the LV (130 ± 13, $n = 73$ pixels). The lateral segment demonstrated a mean similarity value of 170 ± 22 ($n = 123$ pixels) identical to that of the LV in the normal patient (170 ± 15, $n = 194$ pixels).

When there are limitations in evaluating areas of 3D superimposition of abnormal contractions as well as the effects of the inter- and intra-ventricular conduction defects, a box-plot display is proposed (Fig. 6). This plotting can be interpreted to represent the severity of the contraction abnormalities. A similarity degree of 100 is used as the reference value. Fig. 6 shows that the median value of the normal patient is significantly greater than that of the other patients. The median value in patients 1 and 3 are in the middle of the box. This indicates that the similarity values distributions are symmetric. Thus, the ventricular contractions are almost homogeneous in these two patients and heterogeneous in the other patients. The outside values, greater than the third quartile, are either very slightly spaced or merged. This expresses the fact that the lateral segments of the five patients are normally contracting ones. All the values do not exceed the value $+200$ which corresponds to a maximal similarity. The outside values, less than the first quartile, are composed essentially, in pathological patients, of two subsets of similarity values. The first subset, starting from the lower fence, is homogeneous. In patient 4, this subset corresponds to an akinesis of the inferoapical segment of the LV. The second subset, separated from the first one, corresponds to a dyskinesis of the distal septum segment. In patients 2, 3 and 5, this subset corresponds to an hypokinesis in the septal, anteroseptal and the distal septal segments, respectively.

There is an obvious relationship between the function of both ventricles. Thus, to characterise the ventricles synchronism, the Gaussian fitted histograms of the similarity values calculated in the LV and the RV are studied

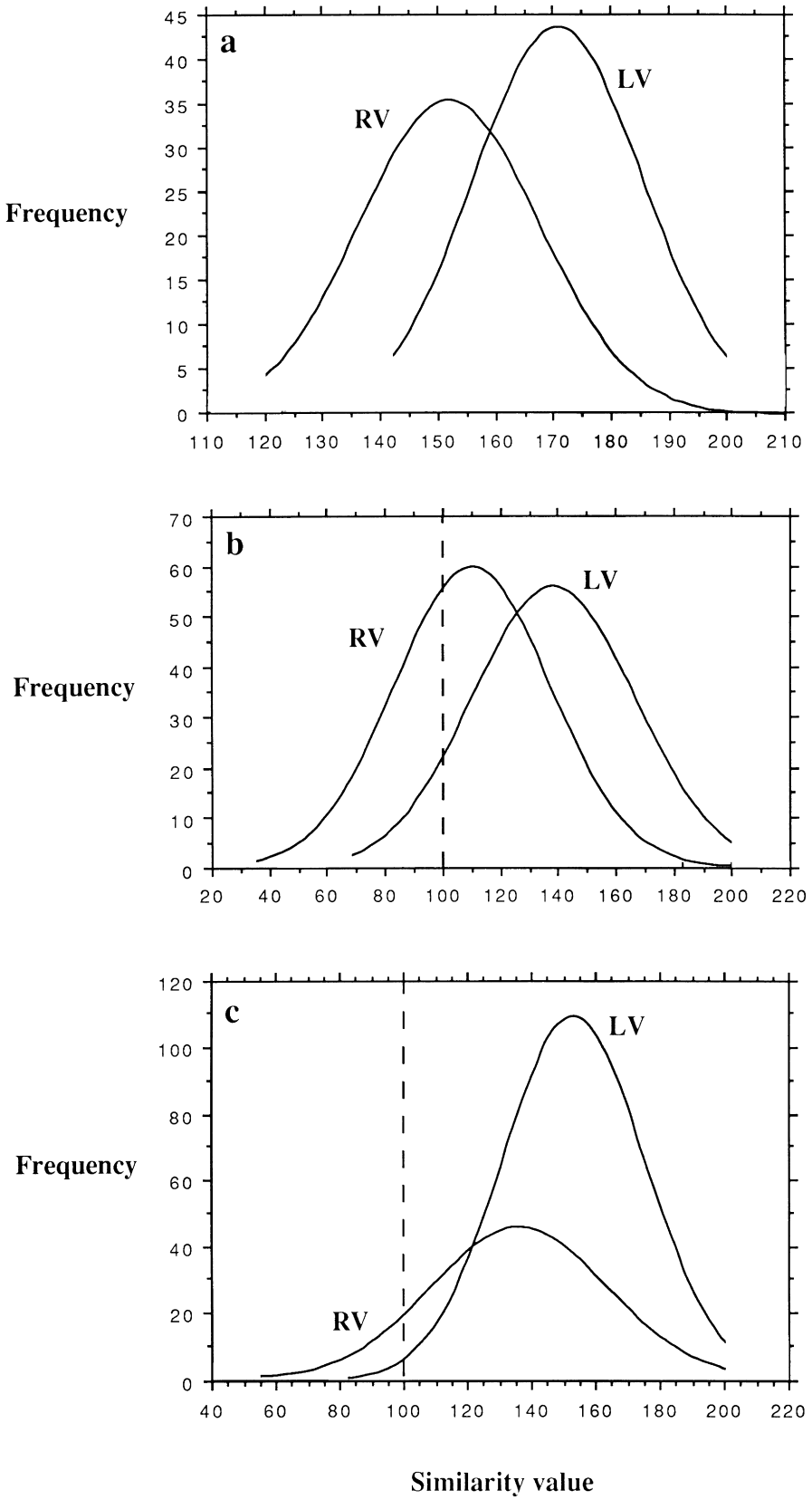

Fig. 7. Gaussian fitted histograms of the similarity values calculated in the RV and the LV for the five patients (1: normal patient; 2, 3, 4 and 5: pathological patients). (Continued overleaf).

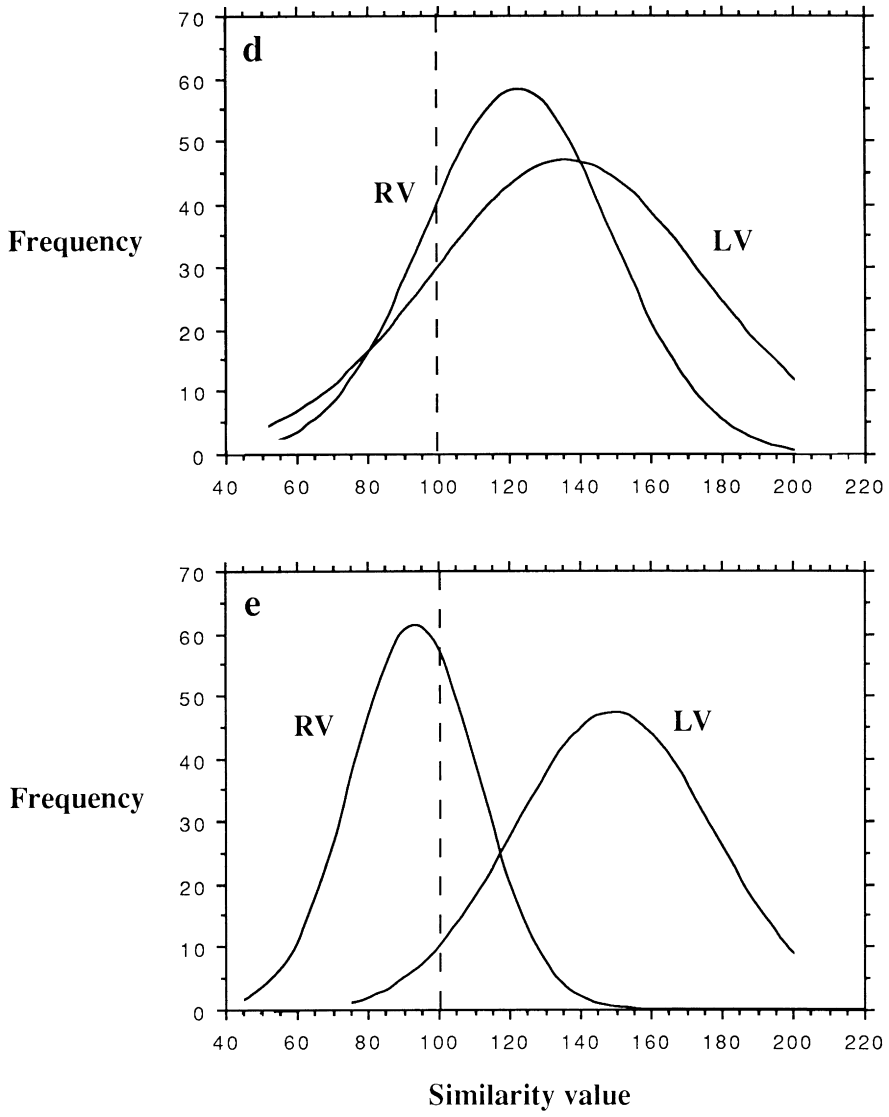

Fig. 7. (*continued*)

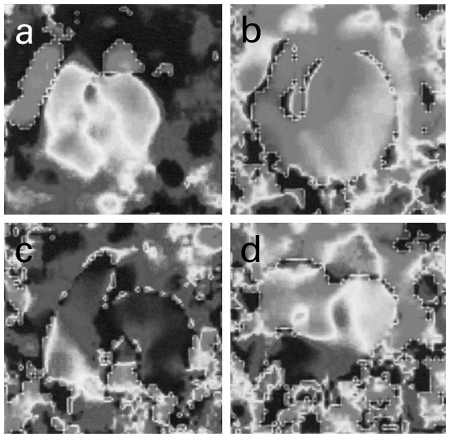

Fig. 8. Phase images (a–d) of the four pathological patients (patients 2–5).

(Fig. 7). These histograms are represented by their mean value and their dispersions. The difference between the mean values of the ventricles, Δm, and the similarity standard deviations of these histograms (σ_{LV}, σ_{RV}) are parameters to describe the synchronism. Thus, a synchronism is characterised by both low Δm and dispersions. For example, the synchronism of the ventricles in patient 1 is defined by the $\Delta m = 20$ and the dispersions $\sigma_{LV} = 17.5$ and $\sigma_{RV} = 14.1$ (Fig. 7(a)). This figure is representative of synchronised ventricles. In patient 5 (Fig. 7(e)) there is a significantly lesser overlap of the two histograms than in the other patients. In all cases, the Gaussian mean value of the LV is greater than that of the RV. This is expected since the LV has a higher similarity because the reference region is defined by an ROI in the LV. Patient 4, presenting a Δm of 13 corresponding to a larger histograms overlapping, has the greatest dispersion value $\sigma_{LV} = 38.5$ for the LV and a low

dispersion $\sigma_{RV} = 19.2$ for the RV (Fig. 7(d)). These findings indicate that the ventricles are asynchronous. This is expected because the LV exhibits three regions with different contraction values: a septal segment normally contracting, a distal septum paradoxically contracting and an akinetic inferoapical segment. Thus, a wider histogram is indicative of a large contraction heterogeneity of the ventricle. Notice that patient 4 exhibits a more important overlap than the normal patient. In Fig. 7(e), there is a large separation of the two histograms, indicating an asynchronism of the ventricles. This result is expected since the mean value in the LV is significantly different from that in the RV which exhibits a high contraction heterogeneity. Compared to patients 1, 4 and 5, patients 2 and 3 (Fig. 7(b) and (c)) have an intermediate degree of asynchronism.

The temporal information giving by the covariance map is compared to that of the phase image. The phase images obtained in four pathological patients (patients 2–5) are shown in Fig. 8. Compared to the results presented in Fig. 5, Fourier analysis (first harmonic) confirms our findings. Note that the ventricular and atrial regions are not well delineated (Fig. 8) as in the covariance analysis (Fig. 5).

4. Discussion

We have developed and implemented the covariance method as a new technique to analyse sequences of nuclear cardiac images. In covariance maps, corresponding to ventricular and atrial ROIs, one recognises the L-shape of the RV. The covariance map may be viewed as a combination of phase and amplitude images generated by Fourier analysis. A careful examination of this map shows that the covariance effect is similar to that of a spatio-temporal filtering. Indeed, the ventricles are well separated from the atria and their edges are well delimited. The advantage of this pseudo-filter is that it is auto adaptable. These two cardiac structures are not identified and separated in the normal patient with the reference placed in the background or in the liver. This is expected because these two ROIs are static regions relatively to cardiac structures. However, we have noted that in 15 patients with hot livers, these two structures are also well recognised and delineated.

The four temporally different ROIs of patient 1 placed in the end diastolic image, which is the first image in the series, have been selected. This is done manually except the LV ROI which is placed automatically, considering that the highest countings are found in the LV region [8]. Thus, a window of 5×5 pixels size with the pixel of maximum intensity as a centre is constructed. One can generate as many parametric images as the number of pixels of the image. To each ROI, corresponds a reference series of mean of pixel values averaged over this ROI. Recall that the scintigraphic images are characterised by both a poor spatial resolution and a high statistical noise. There is no restriction on the amplitude of the mean values calculated to perform a covariance measure. In Fourier analysis, the phase in a constant source image point is not calculated, because it is unreliable when the amplitude of this point is very low. The covariance measure is threshold amplitude independent.

We have shown that the box-plot representation accompanying the covariance leads to a better and more rapid interpretation for decision making. The problems of similarity histogram quantification should not be neglected and special care has to be taken in order to avoid erroneous conclusions from data. The mean values calculated in the ventricles (right or left) can be compared only in a given patient to show an advanced or a delayed contraction. If the similarity values are determined for the range 0–200 covering the whole cardiac cycle (R–R interval), the standard deviation of the histogram may be reproducible. However, due to an unavoidable degree of physiological arrhythmia, frames corresponding to the end of cycle (diastasis) generally show a drop of activity (called drop of the tail of the curve). If the cardiac cycle is shortened by one or several frames to eliminate the last part of the curve, this operation acts as a zoom on the similarities histogram and its standard deviation automatically increases in the same proportion as the cardiac cycle is shortened. In practical cases, the shape of the histogram may be different from normality (Gaussian). This shape is sometimes bimodal if a normal contraction region coexists with an abnormal region in the same ventricle with crisp separation. Therefore the standard deviation of the similarity values can only be considered as an indicator of contraction heterogeneity without the possibility of distinction between a continuous spectrum of contraction times or a juxtaposition of two near homogeneous, but different, zones. In cases of arrhythmias or conduction abnormalities (Wolf–Parkinson–White syndromes for instance) some care has to be taken since similarity delays may be the results of activation abnormalities with unaltered contraction, contraction abnormalities with normal activation or a combination of both.

The Fourier analysis is limited to a first harmonic. Pixels with negligible amplitude are not represented in the phase map as these pixels are usually static structures. A mask that includes the pixels with amplitude less than 15% of the maximum value in the image is used to skip such pixels. This thresholding is the only one pre-processing of the phase image. For better comparison of our method and the Fourier analysis the phase map has not been post-processed. Note that the Covariance method is performed without post- or pre-processing. Qualitatively, results are better with the covariance method (Fig. 5) than with Fourier analysis (Fig. 8). For example, the akinesis of the inferior part of the RV (patient 5) (Fig. 5(d)) or akinesis of the inferoapical of the LV (patient 4) (Fig. 5(c)) are better revealed than in Fig. 8(c) and (d), respectively.

5. Conclusion

A method to analyse nuclear cardiac images acquired throughout the cardiac cycle is proposed. Similarity measure, using the covariance function, between time activity curve of each pixel and a fixed reference is calculated. The generated covariance map is nothing but a representation of the temporal similarity of the pixels to the fixed reference. The method uses the information from the whole cardiac cycle and consequently has much better signal-to-noise ratio than a method based on pairs of frames. Thus, the original data contained in sixteen images are reduced to one static image which is a descriptor of heart function. A box-plot representation is proposed for better interpretation. The method has been applied to various series of nuclear cardiac images. The covariance measure clearly separates the atria from the ventricles. In patients with wall motion abnormalities, areas of various contraction abnormalities are recognised and their boundaries delimited. This method is as fast as the Fourier analysis. Despite its simplicity and the small computation time required, covariance method has the disadvantage that it does not take the spatial information of the pixels into account. This method has only been tested on LAO projection series. A large number of pathological cases must be studied to show its reliability for routine clinical use. We have not studied the effect of the window size on the covariance map values. Our results show that the reference placed either in the atrial region or in the LV one is the best condition to assess the distribution of the temporal degree of similarity. Quantitative measurements, such as standard deviation, from covariance map of the homogeneity or heterogeneity of temporal response of the ventricles may be useful to appreciate the severity of ventricular arrhythmias.

References

[1] Jackson SA, Nickerson R, Martin RH, Iies S, Barnes D. Regional observer performance variations in the evaluation of gated cardiac blood pool studies. Eur J Nucl Med 1992;19:254–257.
[2] Goris ML, Briandet PA. A clinical and mathematical introduction to computer processing of scintigraphic images, New York: Raven Press, 1983.
[3] Schad N. Nontraumatic assessment of left ventricular wall motion and regional stroke volume after myocardial infarction. J Nucl Med 1977;18:333–341.
[4] Pavel DG. The diagnostic relevance of an integrated approach to gated cardiac studies. In: Schmidt H, Rosler H, editors. Nuklearmedizin: computer assisted functional analysis, New York: FK Schattauer, 1982. pp. 97–103.
[5] Bossuyt A, Deconinck F, Lepoudre R, Jonckheer M. The temporal Fourier transform applied to functional isotopic imaging. In: Di Paola R, Kahn E, editors. Information processing in medical imaging. INSERM 88, Paris, 1979. pp. 397–408.
[6] Botvinick E, Dunn R, Frais M, O'Connell W, Shosa D, Herfkens R, Scheinman M. The phase image: its relationship to patterns of contraction and conduction. Circulation 1982;65:551–560.
[7] Pavel D, Byrom E, Lam W, Meyer-Pavel C, Swiryn S, Pietras R. Detection and quantification of regional wall motion abnormalities using phase analysis of equilibrium gated cardiac studies. Clin Nucl Med 1983;8:315–321.
[8] Boudraa AE, Mallet JJ, Besson JE, Bouyoucef SE, Champier J. Left ventricle automated detection method in gated isotopic ventriculography using fuzzy clustering. IEEE Trans Med Imaging 1993;12:451–465.
[9] Pavel DG, Briandet PA. Quo vadis phase analysis. Clin Nucl Med 1983;8:564–575.
[10] Schwaiger M, Ratib O, Henze E. Diagnostic limitation of phase analysis in severely impaired left ventricular function. J Nucl Med 1982;23:P55 abstract.
[11] Turner DA, Von Behren PL, Ruggie NT. Noninvasive identification of initial site of abnormal ventricular activation by least square phase analysis of radionuclide cineangiograms. Circulation 1982;65:1511–1518.
[12] Barber DC. The use of principal components in the quantitative analysis of gamma camera dynamic studies. Phys Med Biol 1980;25:283–292.
[13] Cavailloles F, Bazin JP, Di Paola R. Factor analysis in gated cardiac studies. J Nucl Med 1984;25:1067–1079.
[14] Cavailloles F, Bazin JP, Pavel D, Olea E, Faraggi M, Frouin F, Di Paola R. Comparison between factor analysis of dynamic structures and Fourier analysis in detection of segmental wall motion abnormalities: a clinical evaluation. Int J Cardiac Imaging 1995;11:263–272.
[15] Faraggi M, Cavailloles F, Assayag P, Benslimene F, Bazin JP. Evaluation des performances de trois méthodes de traitement de l'image scintigraphique de ventriculographie cardiaque a l'équilibre. J Biophysique Biomecanique 1986;12:67–69.
[16] Rogowska J, Wolf GL. Temporal correlation images derived from sequential MR scans. J Comput Assist Tomogr 1992;16:784–788.
[17] Bandettini PA, Jesmanowicz A, Wong EC, Hyde JS. Processing strategies for time course data sets in functional MRI of the human brain. Magn Reson Med 1993;30:161–173.
[18] Barnea DI, Silverman HF. A class of algorithms for the fast digital image registration. IEEE Trans Comput 1972;21:179–186.
[19] Pratt WK. Digital image processing, New York: Wiley, 1978.
[20] Tanimoto TT. A nonlinear model for computer assisted medical diagnostic procedure. NY Acad Sci Trans 1961;23:576–578.
[21] Venot A, Lebruchec JF, Roucayrol JC. A new class of similarity measures for robust image registration. Comput Vision Graphics Image Proc 1984;28:176–184.
[22] Wagner R, Galiana HL. Evaluation of three template matching algorithms for registering images of the eye. IEEE Trans Biomed Engng 1992;39:1313–1319.

Abdel-Ouahab Boudraa graduated from the Institute of Physics, Constatine University, Algeria, in 1987. He received a University degree in Nuclear Magnetic Resonance in 1993, a PhD degree in Biomedical Engineering in 1994 and University degrees in Statistics and Modeling in 1995 and Positron Emission Tomography in 1997 all from the University of Claude Bernard, Lyon 1, France. In 1998, he joined the University Paris 13 (Institut Galilée) where he is currently an Associate Professor of Electrical Engineering. His current research interests include computer vision, vector quantisation, data structures and analysis, hard and fuzzy pattern recognition and applications of fuzzy set theory to medical image. Dr Boudraa is an Associate Member of the IEEE Society.

Jacques Champier received a PhD degree in Biochemistry and Molecular Biology in 1979 from the University of Lyon, France. He is currently Research Engineer at the University Claude Bernard of Lyon. He teaches Geometric Optics at RTH Laennec Medical School. His research interests include image processing and biological telemetry.

Mourad Djebali is Associate Professor at the Laboratoire d'Informatique Graphique Image et Modélisation (L.I.G.I.M), Claude Bernard University, Lyon 1, France. He received a PhD in Computer Science from Claude Bernard University, Lyon 1, France. His research include computer vision, computer aided-design and pattern recognition.

Faiza Behloul was born in Algiers, Algeria on October 14, 1971. She received her engineering degree in Computer Science from the National Institute of Computer Science of Algiers in 1993 and received her PhD degree in 1999 from INSA of Lyon. She is currently at the Division of Image Processing, at Leiden University Medical Center. Her current research interests include knowledge based image processing, data fusion and soft computing.

Azeddine Beghdadi graduated from the Institute of Physics, ES-Senia University, Oran, Algeria, in 1979, and received the D.E.A. in optics from the University Paris 11 in 1983 and his PhD degree in optics and signal processing from the University Paris 6 in 1986. He is currently Associate Professor at the University Paris 13 and researcher at L2TI laboratory in Villetaneuse, France. His research interests include low-level image treatments (enhancement, segmentation, nonlinear filtering), image quality assessment, visualisation/compression of 3D-medical images and physics-based and biology-based models for image processing. Dr Beghdadi is Member of the IEEE and EURASIP.